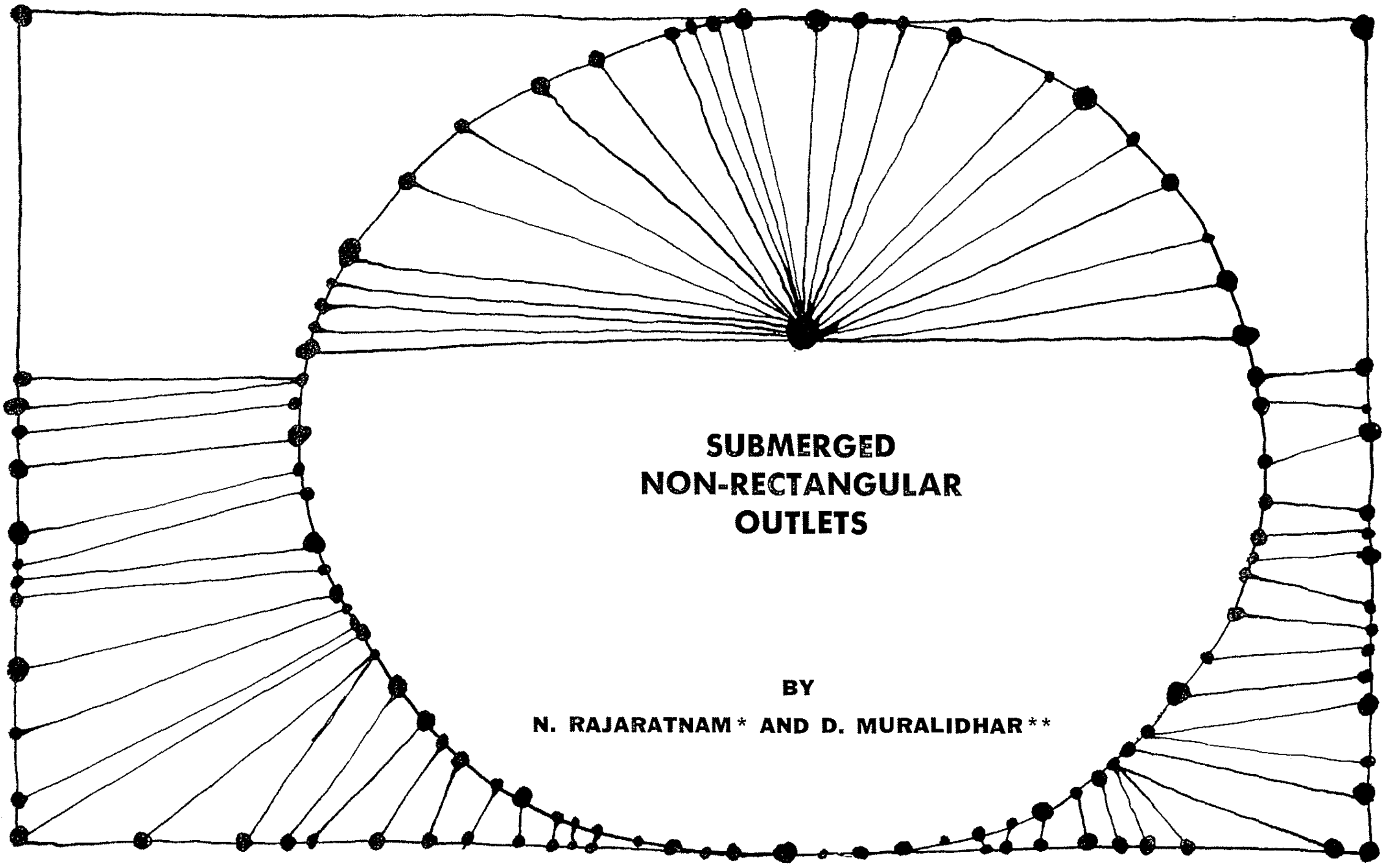

SUBMERGED NON-RECTANGULAR OUTLETS

BY

N. RAJARATNAM * AND D. MURALIDHAR **

Introduction

Hydraulic structures like river and canal outlets and culverts sometimes work under submerged conditions. For designing safe but economical energy dissipators for these outlets structures, it is necessary to have a good knowledge of at least the mean flow characteristics below them. If the outlet jet is far removed from the confining boundaries, it could be analysed as a free turbulent jet [1, 5, 13] (1). If it occupies the full width of the downstream channel and issues tangential to its bed, then it could be treated as a plane turbulent wall jet [4, 5, 6, 11]. If the full-width jet has an abrupt drop at the entrance, the flow could be analysed as a plane turbulent reattached wall jet [8]. If it is a part-width jet with no drop, it could be analysed as a restricted form of three dimensional wall jet [7]. The case of part-width rectangular jets with drop has recently been studied by Rajaratnam and Muralidhar [10]. This paper presents the results of an experimental study of the diffusion below certain non-rectangular outlets under submerged flow conditions.

Experiments and results

The experiments were conducted in a rectangular flume 18 inches wide, 36 inches deep and 16 feet long with smooth bed and side walls. A detailed description of the experimental arrangement could be found in [8]. The non-rectangular shapes studied included basically a triangle, semi-circle, circle and some variations of the above which are shown in Figure 1.

With the exception of the circle, all the other outlets were short conduits and had a lengths of about 30 inches. The circular outlet was a nozzle with an area ratio of about 2.8 and a length of transition of 10 inches. On the whole, nine series of experiments were made and the important details of these experiments are given in Table 1. In Table 1, B is the width of the downstream rectangular channel, b is the characteristic width and h_0 is the height of the outlet, U_0 and U_a are respectively the maximum and average velocities at the outlet, r' is the characteric length of the outlet defined as the ratio of the area to the fluid boundary perimeter of the outlet jet and h is the height of abrupt drop at the efflux section.

On the whole 24 experiments were conducted. In all these experiments, the mean velocity distribution in the forward flow in the central plane of the outlet was measured by means of a 3 mm external diameter Prandtl-type Pitot-static tube. The average outlet velocity U_a was obtained by dividing the measured discharge by the outlet area and the maximum velocity U_0 was obtained by making a velocity traverse as close as possible to the efflux section. In the first two series, the centerline bed shear stress was measured by means of a

* M.A.S.C.E., Assoc. Prof., Department of Civil Engineering, University of Alberta, Edmonton, Canada.
** Research Assoc., Department of Civil Engineering, University of Alberta, Edmonton, Canada.
(1) Numerals in parentheses refer to corresponding items in the References.

Article published by SHF and available at http://www.shf-lhb.org or http://dx.doi.org/10.1051/lhb/1969004

3 mm external diameter Preston tube [2, 3]. All these experimental data are presented and discussed in the following sections of this paper.

Triangular outlets

For all the triangular shapes tested, the vertex angle was kept at about 90 degrees. If b is the base width of the triangle, with its base sitting on the bed, the ratio b/B was varied from 0.224 to 0.826. Figure 2 shows a typical centerplane velocity distribution in which u is the turbulent mean velocity at a normal distance of y from the bed and x is the longitudinal distance from the outlet. From Figure 2, it is seen that the almost-symmetrical parabolic velocity distribution at the efflux section transforms to that of a wall jet at x greater than about 21.0 inches.

The wall jet profiles of the first series are tested for similarity in Figure 3, in which u/u_m is plotted against $\eta = (y/\delta_1)$ where u_m is the maximum value of u at any section and δ_1 is the value of y where $u = (u_m/2)$ and $\partial u/\partial y$ is negative. Sometimes u_m and δ_1 are referred to respectively as the velocity and length scales. Figure 3 shows that the velocity distribution for all the five runs of the first series agree fairly well with that of the classical wall jet, that is, the plane turbulent wall jet growing on a smooth boundary in an infinite expanse of the same fluid under zero pressure gradient.

The variation of the velocity and length scales are studied in Figure 4. In Figure 4 a, u_m/U_0 is plotted against x/r' along with the curves of the classical wall jet, denoted as CWJ and of the rectangular wall jet in wider channels, denoted as WJWC. The present data lie somewhat lower than the above two curves and a dotted line has been drawn to represent the same. The length scale data in Figure 4 b is described fairly well by the WJWC curve for x/r' up to about 40 beyond which they approach the CWJ curve.

Figure 5 a shows few typical variations of the centerline bed shear stress τ_0. A dimensionless plot of the variation of the shear stress is shown in Figure 5 b, in which τ_{0m} is the maximum value of τ_0 and θ is the value of x, where $\tau_0 = \tau_{0m}/2$ and a single curve could reasonably be drawn for all the five experiments of the first series. It was found that the shear stress scale τ_{0m} could be taken as equal to $0.0044\ \rho U_0^2/2$ and the length scale θ was found to be equal to about 26.2 r'.

Semicircular outlets

Four experiments were done with the semicircular shape and with its diameter as the base width b, the ratio b/B was varied from 0.22 to 0.67. A typical velocity distribution is shown in Figure 6, which shows the initial parabolic distribution gradually changing to that of a wall jet. The velocity distribution data are tested for similarity in Figure 7. It is found that for the first experi-

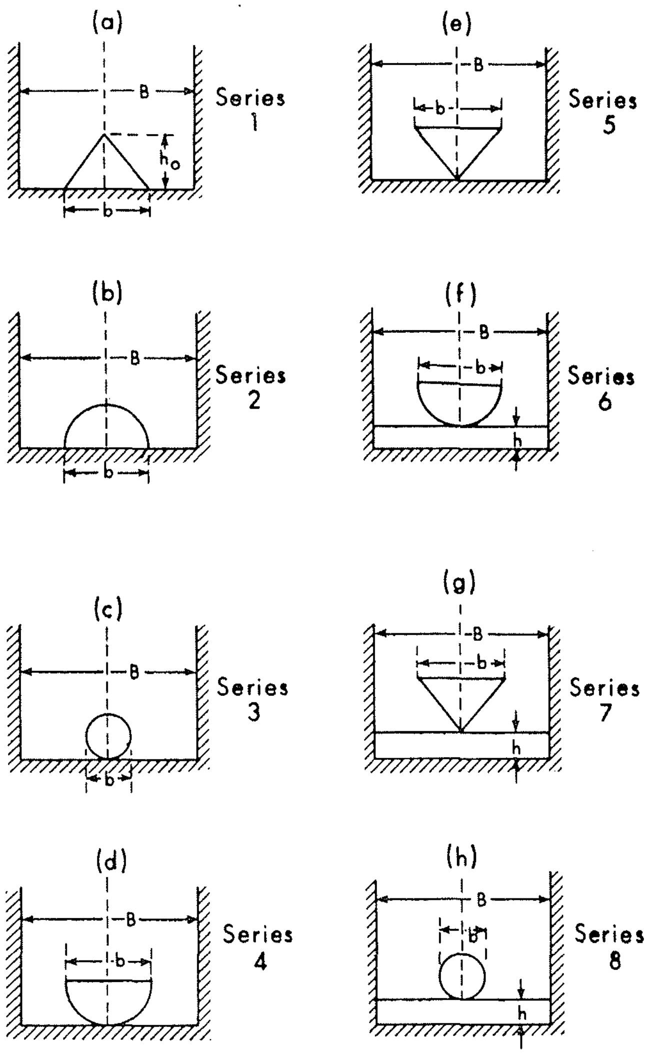

1/ Non-rectangular outlet shapes studied.
Orifices non rectangulaires étudiés.

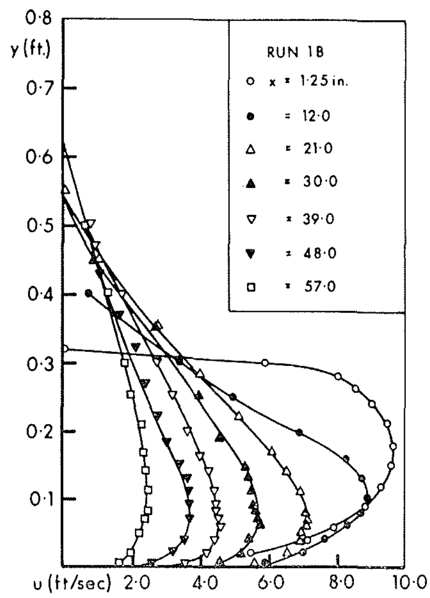

2/ Typical velocity distribution (triangular outlets).
Répartition type des vitesses (orifices triangulaires).

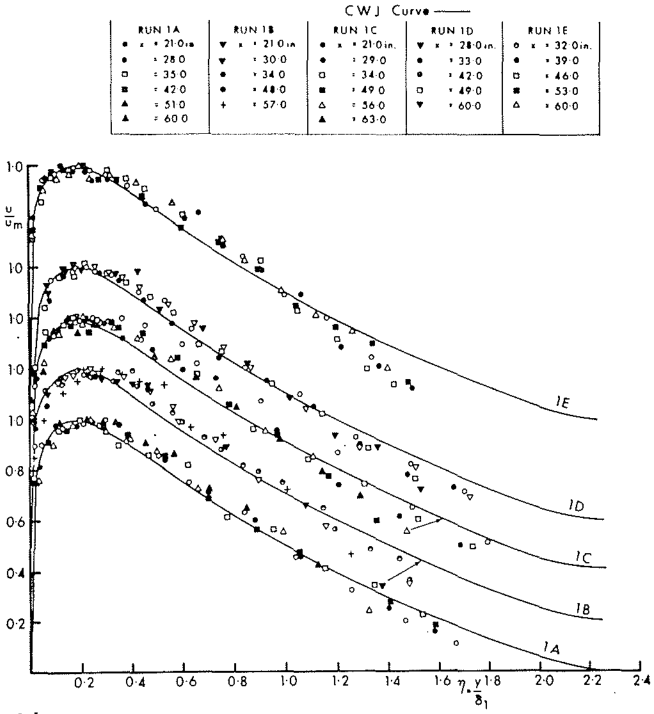

3/

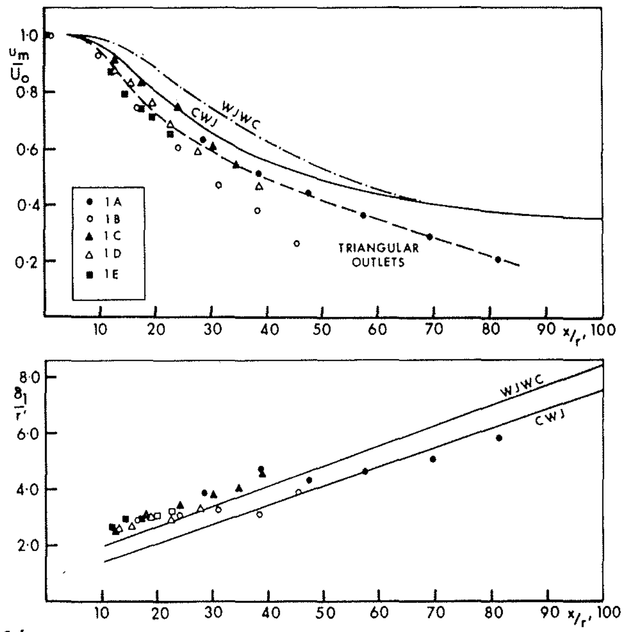

4/

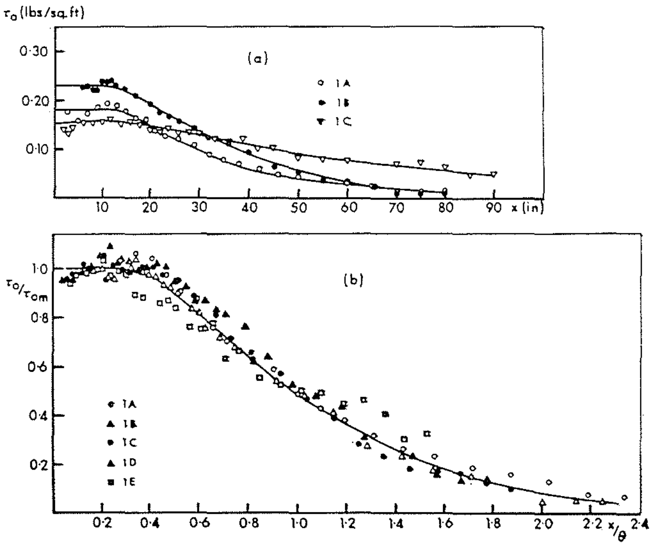

5/

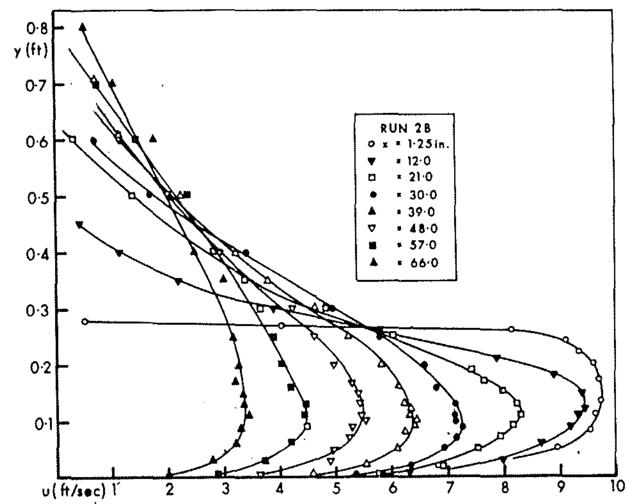

6/

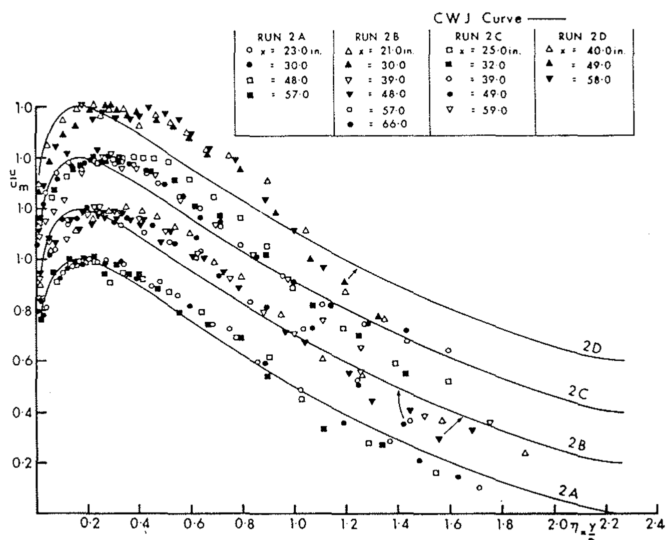

3/ Velocity distribution. Similarity plot (triangular outlets).
Répartition des vitesses. Similitude des courbes.

NOTE. — The origin has been vertically shifted for each curve / *Les origines des courbes ont été déplacées dans le sens vertical.*

4/ Velocity and length scales (triangular outlets).
Echelles des vitesses et des longueurs (cas des orifices triangulaires).
WJWC : jet de paroi dans les canaux de plus grande largeur.
CWJ : jet de paroi classique.

5/ Bed shear stress studies (triangular outlets).
Etudes de la contrainte de cisaillement au fond (orifices triangulaires).

6/ Typical velocity distribution (semicircular outlets).
Répartition type des vitesses (cas des orifices semi-circulaires).

7/ Velocity distribution. Similarity plot (semicircular outlets).
Répartition des vitesses. Similitude des courbes (orifices semi-circulaires).

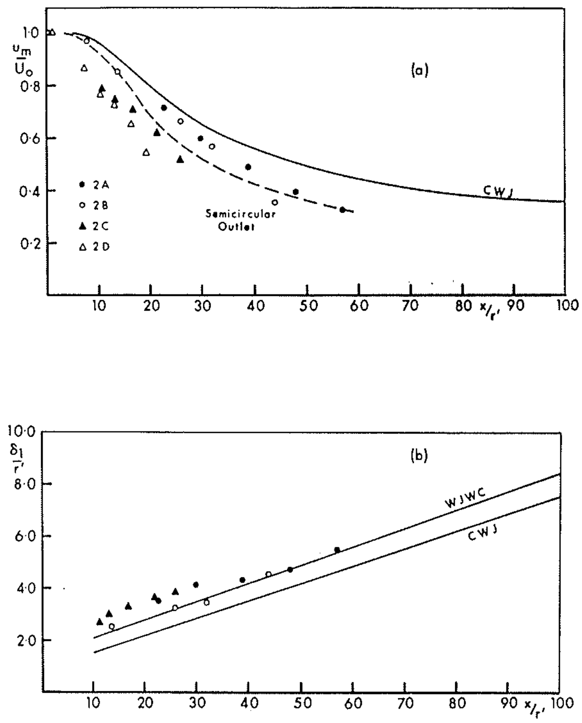

8/ Velocity and length scales (semicircular outlets).
Echelles des vitesses et des longueurs (orifices semi-circulaires).

ment, the data agree fairly well with that of the classical wall jet, whereas for the other three experiments, especially the fourth one, the data indicate that the velocity profiles are not yet fully developed. It is believed that for sufficiently large values of x, the velocity distribution data would agree with that of the classical wall jet.

The variation of the velocity scale is studied in Figure 8 *a*, and the mean curve for the semicircular outlets is somewhat lower than the curves of the CWJ and WJWC. The length scale data for the first three runs, shown in Figure 8 *b* agree fairly well with the WJWC line. A study of the center-line bed shear stress data for the semicircular outlets was made and these data agreed well with the results of the triangular outlets.

Circular outlets

The circular outlet was provided by a nozzle of 3.05 inches diameter and only two experiments were done. The typical velocity distribution in Figure 9 shows that here again the forward flow in the centerplane behaves like a plane wall jet. The dimensionless plot of Figure 10 confirms the above observation. Figure 11 *a* shows that the velocity scale data agree well with the curve of the WJWC but the length scale data in Figure 11 *b* lie somewhat higher than the curves of the CWJ and WJWC.

Inverted semicircular and triangular outlets

Two experiments were done, one each with an inverted semicircle (run 4 *a*) and an inverted triangle (run 5 *a*), sitting on the bed of the channel. In both the cases, for sufficiently large values of x, the velocity distribution is described well by the curve of the CWJ, as could be seen from the lower-most curves of Figures 12 and 13. The variation of the velocity scale is studied in Figure 14 *a* where it is seen that for both these inverted shapes, the data agree fairly well with the curve of the WJWC. But the length scale variation studied in Figure 14 *b*, shows that for each of these two shapes, the data lie on different curves, distinct from those of the CWJ and WJWC.

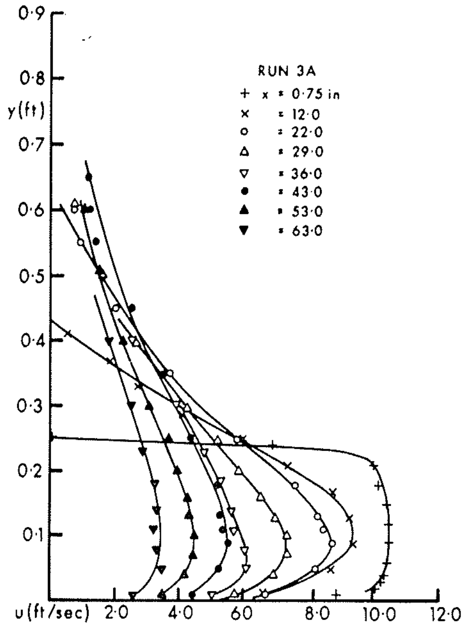

9/ Typical velocity distribution (circular outlets).
Répartition type des vitesses (orifices circulaires).

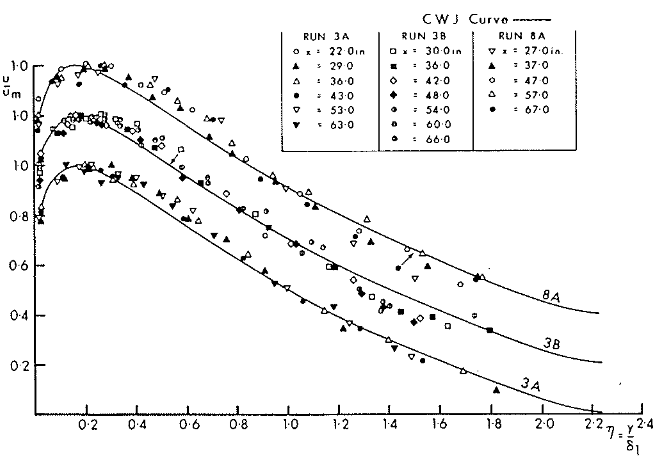

10/ Velocity distribution. Similarity plot (circular outlets).
Répartition des vitesses. Similitude des courbes (orifices circulaires).

Inverted semicircular and triangular outlets with abrupt drop

For the inverted semicircular and triangular shapes, it was desired to study the effect of an abrupt drop at the efflux section on the forward flow velocity distribution. For the semicircular outlet of basic width of 6.0 inches, the height of the drop was made equal to 1.03, 2.42 and 3.42 inches (runs 6 *a*, 6 *b* and 6 *c*). The velocity distribution measurements, plotted in the conventional dimensionless manner in Figure 12, shows that for all these runs, the distribution in the reattached flow agrees (of course, with some scatter) with the curve of the classical wall jet. But in the case of the inverted triangular outlet with the drop height equal to 0.97, 2.50 and 3.58 inches (runs 7 *a*, 7 *b* and 7 *c*), the velocity distribution in the reattached forward flow differed greatly from that of the CWJ as could be seen from Figure 13.

In Figure 15 *a*, the velocity scale data has been plotted for these two shapes and a mean curve is drawn, which is much lower than the curves of the CWJ and WJWC for x/r' greater than about 40. In Figure 15 *b*, the length scale data for only the semicircular outlet are shown and their variation appears to be very complicated. The corresponding data for the inverted triangle are not studied since the velocity distribution was considerably different from that of the classical wall jet.

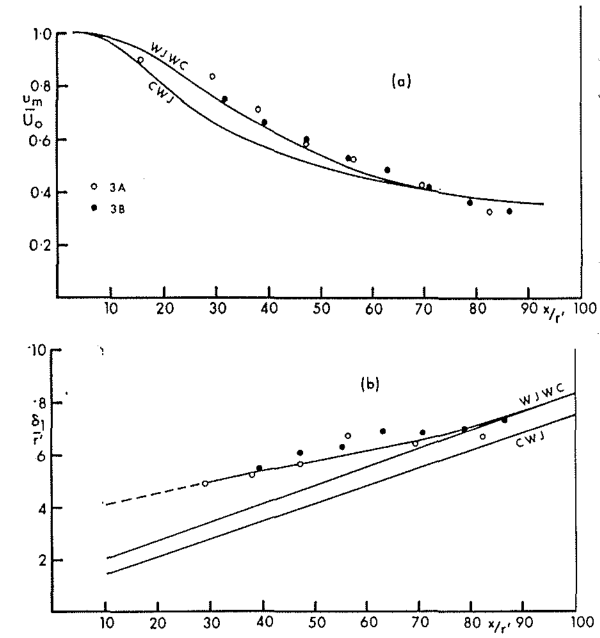

11/ Velocity and length scales (circular outlets).
Echelles des vitesses et des longueurs (orifices circulaires).

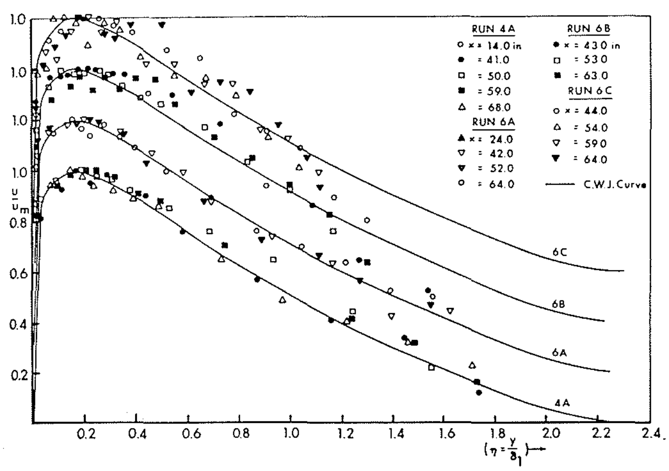

12/ Velocity distribution. Similarity plot (inverted semicircle).
Répartition des vitesses (cas du demi-cercle inversé).

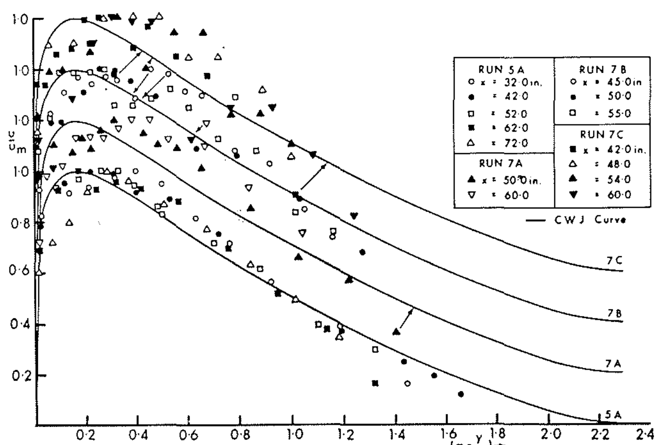

13/ Velocity distribution. Similarity plot (inverted triangle).
Répartition des vitesses. Similitude des courbes (triangle inversé).

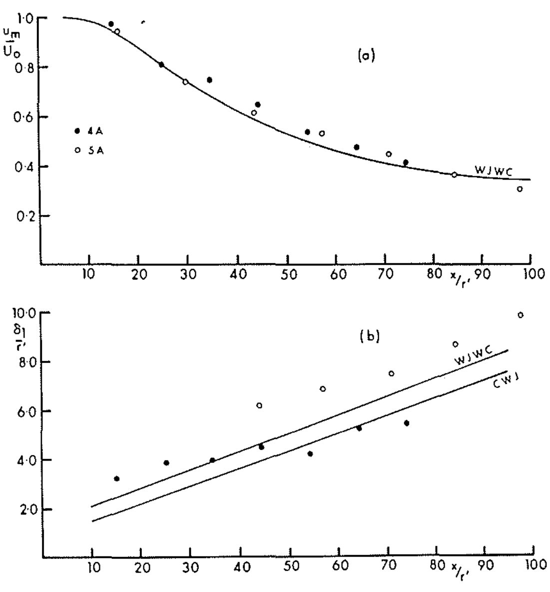

14/ Velocity and length scales (inverted semicircle and triangle).
Echelles des vitesses et des longueurs (cas du demi-cercle et du triangle inversés).

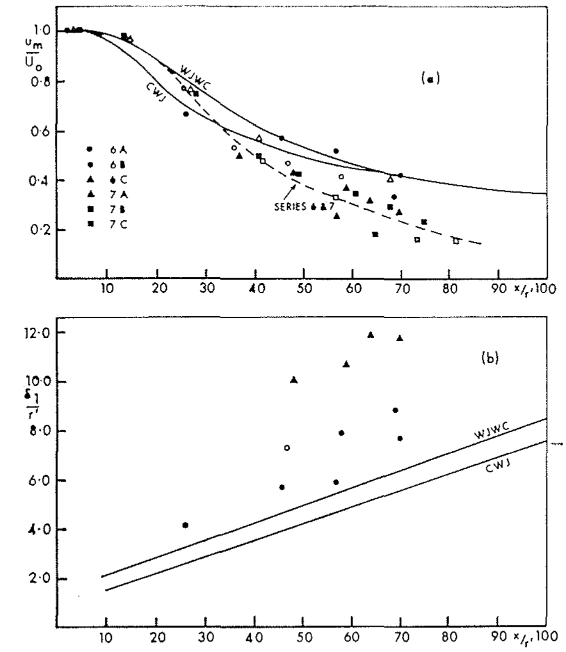

15/ Velocity and length scales (inverted semicircle and triangle with drop).
Echelles des vitesses et des longueurs (cas du demi-cercle et du triangle inversés, avec chute).

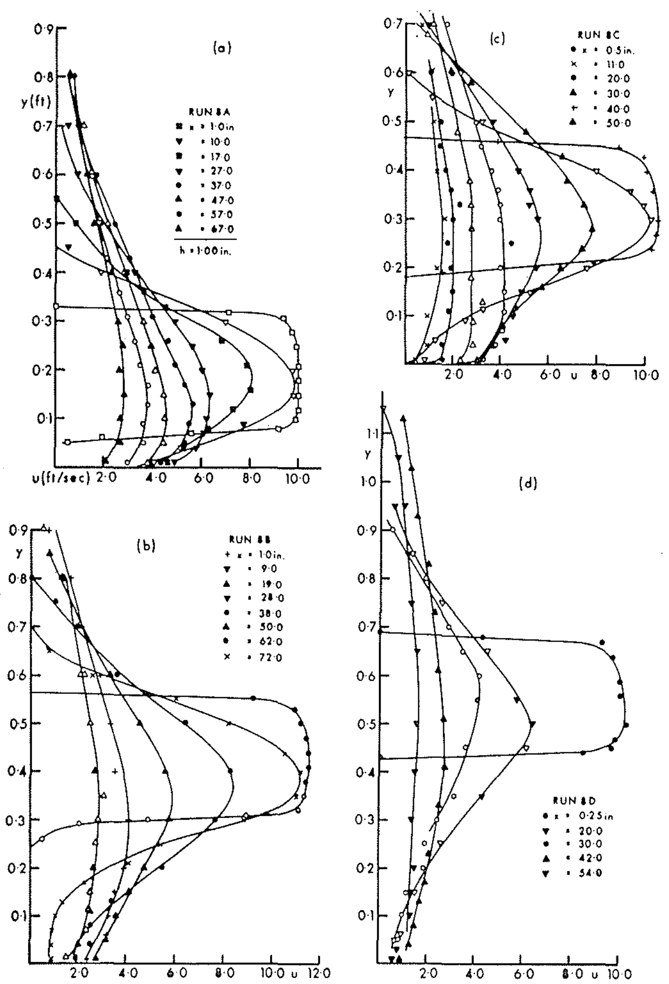

16/ Circular outlets with drop. Velocity distribution.
Orifices circulaires avec chute. Répartition des vitesses.

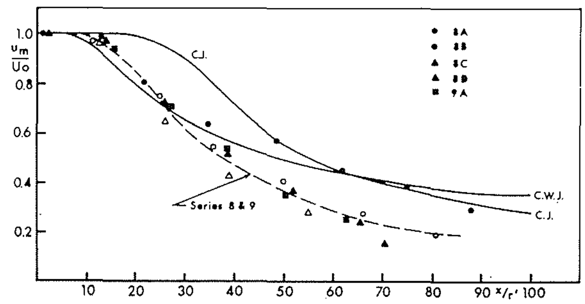

17/ Velocity scales (circular outlets with drop).
Echelles des vitesses (orifices circulaires avec chute).

Circular outlets with abrupt drop

The circular nozzle was tested for four values of the drop height equal to 1.0, 2,60, 3.60 and 5.08 inches (runs 8 *a*, 8 *b*, 8 *c* and 8 *d*) and the last experiment was conducted with a circular pipe outlet of the same diameter with a drop height of 2.10 inches. The velocity distribution patterns of these experiments (series 8), plotted in Figure 16 (*a* to *d*), show qualitatively that as the height of drop increases, the velocity distribution in the centerplane of the forward flow changes from that of a plane wall jet to the circular free jet. The maximum velocity u_m at different sections for these

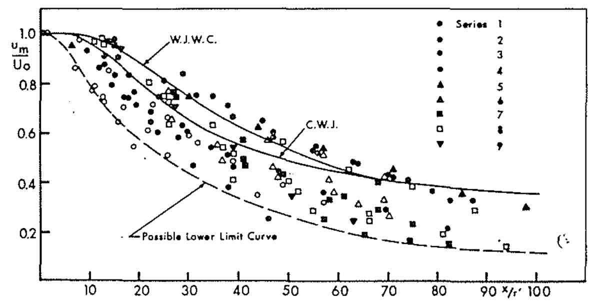

18/ General plot. Velocity scale.
Courbes générales. Echelle des vitesses.

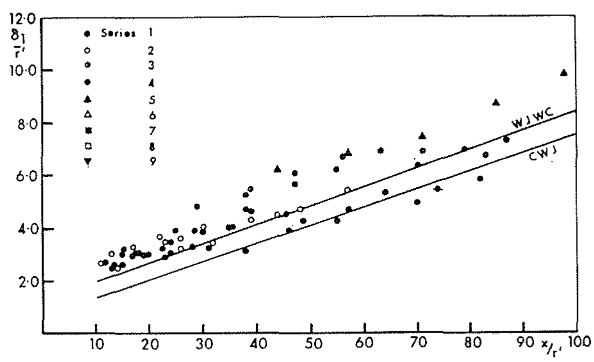

19/ Length scale. (Non-rectangular outlets).
Echelle des longueurs (orifices non rectangulaires).

runs has been studied in Figure 17 and a mean curve has been drawn. Figure 17 also shows the corresponding curve of the circular free turbulent jet and it is interesting to see that the present data lie (mostly) much lower than the curves of the CWJ and the circular jet, denoted as CJ.

General discussion

In the preceding sections of this paper experimental results have been presented concerning the diffusion below certain non-rectangular outlets. For the present, confining the discussion to the non-rectangular outlets without a drop at the efflux section, it could be said that in general the velocity distribution in the centerplane (for x greater than about $12\,r'$) agrees with that of the classical wall jet. This indeed is an interesting observation. Secondly, regarding the velocity scale, the variation for each particular shape seems to be different and the data for all the runs are shown together in Figure 18. It is seen from Figure 18 that the data is roughly contained by the WJWC curve on top and a possible lower limit curve is also shown. Similarly, the length scale data for all the non-rectangular outlets is shown in Figure 19 and for certain preliminary design purposes, the WJWC curve itself could be assumed to represent the data over the range studied.

With these observations, it should be possible to predict the mean velocity distribution in the centerplane below submerged non-rectangular outlets. The centerplane is believed to be plane of maximum velocity. Further studies regarding the flow characteristics on either side of the centerplane have to be made. The bed shear stress distribution on the bed should also be studied for all these shapes. If these outlets are located with an eccentricity with respect to the centerline of the downstream channel, using the results of [10], it could be predicted that the effects of eccentricity on the velocity distribution, velocity and length scale would be small. In the case of non-rectangular outlets with an abrupt drop, only some preliminary results have been obtained. The exploratory experiments with the circular nozzle for four heights of drop indicate that it would be very interesting to study the transformation of the plane wall jet profile to that of the circular free jet, as the height of drop increases continuously from zero.

Another result of practical value is that for the non-rectangular outlets studied, the ratio of the average to maximum velocity at the efflux section is about 0.84.

Conclusions

Based on the experimental results presented in this paper, the following conclusions could be drawn.

For the submerged non-rectangular outlet shapes studied, when there is no drop at the efflux section, the forward flow velocity distribution in the centerplane of the outlet could satisfactorily be described by the corresponding curve of the classical wall jet, beyond a certain minimum distance from the outlet equal to about 12 times the characteristic length r'. The length scale could be predicted fairly well using the curve of the rectangular wall jet (i.e. WJWC). But the velocity scale data varies in a distinct manner for each shape, which could be obtained from the corresponding figure. The centerplane bed shear stress has been studied only for the triangular and semicircular outlets. When there is a drop at the efflux section, the flow becomes more complex and only some exploratory results have been obtained.

Acknowledgements

The work reported in this paper was conducted in the Hydraulics Laboratory of the Civil Engineering Department of the University of Alberta, Edmonton and the authors are thankful to the National Research Council of Canada for the financial assistance provided.

TABLE 1

Non-rectangular outlets (experimental details)

Run No.	B_{in}	b_{in}	h_{oin}	b/B	r'_{in}	U_* ft/s	U_* ft/s	h_{in}
1a	18.0	4.03	2.09	0.224	0.73	6.29	9.13	zero
1b	18.0	7.07	3.60	0.394	1.25	7.58	8.93	zero
1c	18.0	9.00	4.60	0.500	1.62	7.60	8.53	zero
1d	18.0	12.10	6.10	0.672	2.17	5.92	7.38	zero
1e	18.0	14.90	7.60	0.826	2.67		5.42	zero
2a	18.0	4.00	2.00	0.222	1.00	7.34	8.46	zero
2b	18.0	6.00	3.00	0.335	1.50	9.00	9.78	zero
2c	18.0	9.00	4.50	0.500	2.25	6.27	8.08	zero
2d	18.0	12.00	6.00	0.667	3.00		6.90	zero
3a	18.0	3.05	3.05	0.169	0.76	8.82	10.43	zero
3b	18.0	3.05	3.05	0.169	0.76	7.62	9.11	zero
4a	18.0	6.00	3.00	0.333	0.92	6.65	7.70	zero
5a	18.0	7.07	3.60	0.394	0.73	6.92	8.53	zero
6a	18.0	6.00	3.00	0.333	1.50	7.71	9.20	1.03
6b	18.0	6.00	3.00	0.333	1.50	7.62	9.05	2.42
6c	18.0	6.00	3.00	0.333	1.50	7.10	8.46	3.48
7a	18.0	7.07	3.60	0.394	0.73	6.32	7.90	0.97
7b	18.0	7.07	3.60	0.394	0.73	7.40	8.93	2.50
7c	18.0	7.07	3.60	0.394	0.73	7.41	9.11	3.58
8a	18.0	3.05	3.05	0.169	0.76	8.77	10.11	1.00
8b	18.0	3.05	3.05	0.169	0.76	9.60	10.44	2.60
8c	18.0	3.05	3.05	0.169	0.76	10.60	11.50	3.60
8d	18.0	3.05	3.05	0.169	0.76	9.43	10.24	5.08
9a	18.0	3.05	3.05	0.169	0.76		9.10	2.10

NOTE: Temperature of water about 70°F.

TABLE 2

Detailed data

Run No.	x_{in}	u_m ft/s	δ_1 ft	x/r'	u_m/U_o	δ_1/r'
1a	0.50	9.13		0.681	1.00	
	21.0	5.77	0.240	28.6	0.632	3.92
	28.0	4.64	0.285	38.1	0.508	4.66
	35.0	3.97	0.260	47.7	0.435	4.25
	42.0	3.26	0.285	57.2	0.357	4.66
	51.0	2.64	0.303	69.5	0.289	4.96
	60.0	1.88	0.356	81.7	0.206	5.82
1b	1.25	9.66		1.0	1.00	
	12.0	8.93		9.6	0.925	
	21.0	7.11	0.304	16.8	0.736	2.92
	30.0	5.75	0.327	24.0	0.595	3.14
	39.0	4.55	0.337	31.2	0.471	3.24
	48.0	3.62	0.326	38.4	0.375	3.13
	57.0	2.42	0.400	45.6	0.251	3.85
1c	1.0	8.53		0.62	1.00	
	21.0	7.80	0.334	12.9	0.914	2.47
	29.0	7.10	0.417	17.9	0.832	3.08
	39.0	6.26	0.462	24.0	0.735	3.41
	49.0	5.16	0.517	30.2	0.605	3.82
	56.0	4.62	0.545	34.5	0.541	4.03
	63.0	3.93	0.618	38.8	0.461	4.57
1d	1.0	7.38		0.46	1.00	
	28.0	6.38	0.464	12.9	0.865	2.56
	33.0	6.10	0.472	15.2	0.826	2.60
	42.0	5.59	0.544	19.3	0.758	3.00
	49.0	5.03	0.532	22.5	0.682	2.94
	60.0	4.29	0.590	27.6	0.581	3.26

Run No.	x_{in}	u_m ft/s	δ_1 ft	x/r'	u_m/U_o	δ_1/r'
3a	0.75	10.50		0.98	1.00	
	12.0	9.43		15.7	0.898	
	22.0	8.77	0.307	28.9	0.835	4.84
	29.0	7.42	0.330	38.1	0.707	5.20
	36.0	6.09	0.357	47.2	0.580	5.62
	43.0	5.48	0.424	56.4	0.522	6.68
	53.0	4.47	0.402	69.5	0.426	6.33
	63.0	3.43	0.422	82.6	0.327	6.65
3b	0.50	9.11		0.66	1.00	
	24.0	6.80		31.5	0.746	
	30.0	6.02	0.345	39.3	0.661	5.44
	36.0	5.48	0.382	47.2	0.601	6.01
	42.0	4.80	0.396	55.1	0.527	6.24
	48.0	4.40	0.435	63.0	0.483	6.85
	54.0	3.80	0.430	70.8	0.417	6.77
	60.0	3.30	0.440	78.7	0.362	6.93
	66.0	3.00	0.460	86.6	0.329	7.25
4a	14.0	7.48	.245	15.3	.973	3.22
	23.0	6.24	.295	25.1	.810	3.87
	32.0	5.75	.304	34.9	.746	3.98
	41.0	4.98	.345	44.7	.648	4.52
	50.0	4.13	.322	54.5	.538	4.21
	68.0	3.16	0.411	74.1	.410	5.40
	59.0	3.67	0.404	64.4	.476	5.30
	1.0	7.70		1.09	1.00	

Run No.	x_{in}	u_m ft/s	δ_1 ft	x/r'	u_m/U_o	δ_1/r'
1e	0.75	6.85		0.28	1.00	
	32.0	5.92	0.602	12.0	0.864	2.71
	39.0	5.42	0.660	14.6	0.792	2.96
	46.0	5.10	0.675	17.2	0.744	3.03
	53.0	4.85	0.673	19.8	0.708	3.02
	60.0	4.41	0.713	22.5	0.644	3.20
2a	0.75	8.46		0.75	1.00	
	23.0	6.01	0.292	23.0	0.711	3.54
	30.0	5.03	0.336	30.0	0.595	4.07
	39.0	4.07	0.357	39.0	0.481	4.33
	48.0	3.26	0.387	48.0	0.386	4.70
	57.0	2.70	0.448	57.0	0.318	5.44
2b	1.25	9.78		0.83	1.00	
	12.0	9.43		8.0	0.965	
	21.0	8.30	0.317	14.0	0.850	2.54
	39.0	6.43	0.398	26.0	0.660	3.18
	48.0	5.50	0.425	32.0	0.562	3.40
	66.0	3.40	0.561	44.0	0.348	4.50
2c	1.0	8.08			1.00	
	25.0	6.28	0.503	11.1	0.776	2.68
	30.0	6.00	0.560	13.3	0.742	2.98
	39.0	5.66	0.627	17.3	0.700	3.34
	49.0	4.95	0.700	21.8	0.612	3.72
	59.0	4.13	0.716	26.2	0.510	3.82
2d	0.63	6.50		0.21	1.00	
	22.0	5.60		7.33	0.860	
	31.0	5.00		10.33	0.77	
	40.0	4.66		13.33	0.716	
	49.0	4.16		16.33	0.640	
	58.0	3.50		19.33	0.540	

Run No.	x_{in}	u_m ft/s	δ_1 ft	x/r'	u_m/U_o	δ_1/r'
5a	0.5	8.53			1.0	
	12.0	8.1		16.4	.95	
	32.0	5.28	0.38	43.6	.619	6.22
	42.0	4.62	0.42	57.4	.541	6.90
	52.0	3.87	0.454	71.0	.454	7.45
	62.0	3.10	0.530	84.5	.364	8.70
	72.0	2.58	.594	98.0	.302	9.75
	22	6.28		30.0	.735	
6a	0.5	9.2		.546	1.00	
	24.0	6.97	.316	26.2	.757	4.14
	42.0	5.22	.43	45.8	.567	5.64
	52.0	4.73	.45	56.8	.514	5.9
	64.0	3.90	.576	69.9	.424	7.56
6b	.50	9.05		0.82	1.00	
	24.0	5.99		26.2	.662	
	33.0	4.79		36.0	.53	
	43.0	4.20	.553	46.9	.464	7.25
	53.0	3.74	.600	57.9	.413	7.86
	63.0	3.00	.670	68.7	.331	8.78
6c	.62	8.46		1.09	1.00	
	34.0	4.16		37.1	.492	
	44.0	3.82		48.0	.416	10.07
	54.0	3.06		58.9	.362	10.74
	64.0	2.20		69.8	.260	11.67
	59.0	2.62		64.4	.309	11.83

— *Non-rectangular outlets*

Run No.	x_{in}	u_m ft/s	δ_1 ft	x/r'	u_m/U_0	δ_1/r'
7a	50.0	3.14	.583	68.0	.398	
	30.0	4.50		40.9	.57	
	62.0	2.00	.72	57.2	.253	
	11.0	7.64		15.0	.966	
	0.5	7.90		.67	1.00	
	20.0	6.00		27.2	.760	
7b	1.25	8.93		1.70	1.00	
	50.0	2.6	.63	68.0	.291	
	30.0	4.40		40.9	.492	
	35.0	3.80		47.6	.425	
	45.0	3.06		61.3	.342	
	10.0	8.61		13.6	.965	
	55.0	2.02	.69	75.0	.226	
	20.0	6.94		27.2	.755	
7c	42.0	2.98		57.2	.326	
	30.0	4.36		40.9	.479	
	0.25	9.11		.34	1.00	
	60.0	1.40		81.7	.153	
	54.0	1.46	0.90	73.5	.160	
	48.0	1.63		65.4	.179	
8a	.50	10.0		0.656	1.00	
	10.0	9.8		13.1	.980	
	17.0	8.02		22.3	.802	
	27.0	6.33	.402	35.4	.633	6.33
	37.0	5.62	.452	48.5	.562	7.11
	47.0	4.47	.476	61.7	.447	7.50
	57.0	3.83	.457	74.8	.382	7.20
	67.0	2.88	.560	87.9	.288	8.82

Run No.	x_{in}	u_m ft/s	δ_1 ft	x/r'	u_m/U_0	δ_1/r'
8b		10.5			1.0	
	9.0	10.2		11.3	.971	
	19.0	7.8		24.8	.745	
	28.0	5.7		36.0	.543	
	38.0	4.2		49.7	.400	
	50	2.8		65.5	.267	
	62	2.0		81.1	.191	
	72	1.50		94.2	.143	
8c	1.5	11.5		1.96	1.00	
	11.0	11.1		14.4	.965	
	20.0	8.30		26.2	.724	
	30.0	5.90		39.3	.514	
	40.0	4.10		52.4	.356	
	50	2.80		65.5	.244	
8d	.25	10.0		.32	1.0	
	10.0	9.6		13.1	.96	
	20.0	6.4		26.2	.64	
	30.0	4.1		39.3	.41	
	42.0	2.80		55.0	.28	
	54.0	1.50		70.6	.15	
9a	1.0	9.10		1.31	1.00	
	21	6.4		27.6	.702	
	12	8.55		15.7	.94	
	30	4.8		39.4	.526	
	39	3.2		51.1	.351	
	48	2.3		63.0	.252	

Notation

The following symbols are used in this paper:

- b width of outlet;
- B width of channel;
- h height of abrupt drop;
- h_0 height of outlet;
- m suffix to denote maximum value;
- r' characteristic length of outlet;
- u turbulent mean velocity;
- u_m velocity scale;
- U_0 maximum velocity at efflux section;
- U_a average velocity at efflux section;
- x longitudinal distance from outlet;
- y normal distance from the channel bed;
- δ_1 length scale for velocity plot;
- η dimensionless ordinate;
- θ length scale for shear stress plot;
- ρ mass density of the fluid;
- τ_0 bed shear stress;
- τ_{0m} maximum value of τ_0.

References

[1] Abramovich (G. N.). — The Theory of Turbulent Jets. English Translation published by M.I.T. Press (1963).

[2] Patel (C. V.). — Calibration of the Preston Tube and Limitations on its Use in Pressure Gradients. *J. of Fluid Mechanics*, vol. 23 (1965), pp. 185-208.

[3] Preston (J. H.). — The Determination of Turbulent Skin Friction by means of Pitot Tubes. *J. of the Royal Aero. Soc.*, London, England, vol. 54 (1954), pp. 109-121.

[4] Rajaratnam (N.). — Submerged Flow Below a Sluice Gate as a Wall Jet Problem. Proc. 2nd Australasian Conf., Auckland, New Zealand (December 1965).

[5] Rajaratnam (N.) and Subramanya (K.). — Three Dimensional Turbulent Jets. *J. of the Royal Aero. Soc.*, London, England (December 1967), pp. 858-859.

[6] Rajaratnam (N.) and Subramanya (K.). — Annotated Bibliography on Wall Jets. Report, Dept. of Civil Engineering, University of Alberta, Edmonton, Canada (1967).

[7] Rajaratnam (N.) and Subramanya (K.). — Diffusion of Rectangular Wall Jets in Wider Channels. *J. of Hydraulic Research*, vol. 5, No. 4, Delft (1967), pp. 281-294.

[8] Rajaratnam (N.) and Subramanya (K.). — Plane Turbulent Reattached Wall Jets. *J. of the Hydraulics Div., Proc. ASCE*, vol. 94, No. HY 1 (January 1968), pp. 95-112.

[9] Rajaratnam (N.) and Subramanya (K.). — Hydraulic Jumps Below Abrupt Symmetrical Expansions. *J. of the Hyd. Div., Proc. ASCE*, vol. 94, No. HY 2 (March 1968), pp. 481-503.

[10] Rajaratnam (N.) and Muralidhar (D.). — Diffusion Below Submerged Rectangular Outlets. Rept., Dept. of Civil Engineering, University of Alberta, Edmonton, Canada (1968).

[11] Schwarz (W. H.) and Cosart (W. P.). — The Two Dimensional Turbulent Wall Jet. *J. of Fluid Mechanics*, vol. 10 (1961), pp. 481-495.

[12] Subramanya (K.). — Turbulent Wall Jets in Hydraulic Engineering. Doctoral Dissertation, Dept. of Civil Engineering, University of Alberta, Edmonton, Canada (1967).

[13] Trentacoste (N.) and Sforza (P. M.). — An Experimental Investigation of Three Dimensional Free Mixing in Incompressible Turbulent Free Jets. *Polytechnic Institute of Brooklyn*, Pibal Rept. 871 (March 1966).

LA HOUILLE BLANCHE A L'ÉTRANGER

Bureaux d'abonnement et de vente

AUSTRALIE

Sydney N.S.W.

GRAHAME BOOK COMPANY : 39-49, Martin Place.

BRÉSIL et AMÉRIQUE DU SUD

Rio de Janeiro

« S.O.G.E.C.O. », José Luis Garcia Renalès : Avenida Rio Branco, 9, Sala 218.

CANADA

Montréal 8.PQ

LIBRAIRIE LEMEAC (Messageries France-Canada) : 371, Ouest Avenue Laurier.

ESPAGNE

Madrid

J. DIAS DE SANTOS : Lagasca n° 38.

Madrid

LIBRERIA VILLEGAS : Preciados, 46.

GRANDE-BRETAGNE

London W.C.2.

W.M. DAWSON & SONS LIMITED : Cannon House, Macklin Street.

London W.1.

I.R. MAXWELL Co. : 4-5, Fitzroy Square.

HOLLANDE

Amsterdam C.

MEULENHOFF & Cie (Librairie) : Beulingstraat, 2-4.

La Haye

MARTINUS NIJHOFF : 9, Lange Voorhout.

HONGRIE

Budapest 62

KULTURA P.O.B. 149.

INDES

Calcutta 16

FRANCE-ARTS, 33-34 Park Mansions, Park Street.

ITALIE

Bologna

TECHNA: Via San Felice, 28, Casella Postale 503.

JAPON

Tokyo

MARUZEN Co. : 6, Tori-Nichome, Nihonbashi, P.O. Box 605.

MEXIQUE

Mexico D.F.

LIBRERIA VILLEGAS MEXICANA : Santa Ma., La Redonda, n° 209-9.

Mexico D.F.

MANUEL BONILLA (Librairie) : Tiber 38-201.

NOUVELLE-ZÉLANDE

Auckland-Wellington C.2.

R. HILL & SONS : Marlock House, 32, Quay Street.

PORTUGAL

Lisboa

LIVRARIA BERTRAND : 73, Rua Garret.

SUÈDE

Stockholm

A.B. HENRIK LINDSTAHLS BOKHANDEL : Odengatan, 22.

SUISSE

Lausanne

S.P.E.S., S.A. Librairie et Editions techniques, 1, rue de la Paix.

TCHÉCOSLOVAQUIE

Praha 2

ARTIA : V° Smeckach, 30.

Praha 1

ORBIS (Import-Export) : Narodin, 37.

TURQUIE

Istanbul

LIBRAIRIE HACHETTE : 469, Istiklal Caddesi, Beyoglu.

U.S.A.

New York

MOORE-COTTRELL SUBSCRIPTION AGENCIES INC. : North Cohocton.

VENEZUELA

Caracas

LIBRERIA VILLEGAS VENEZOLANA, Avenida Urdaneta, Esquina Ibarras, Edificio Riera.